



# Enhancement of viscosity and thermal conductivity of soybean vegetable oil using nanoparticles to form nanofluids for minimum quantity lubrication machining of difficult-to-cut metals

Theodore O. Nwoguh<sup>1</sup> · Anthony C. Okafor<sup>1</sup> · Hilary A. Onyishi<sup>1</sup>

Received: 17 October 2020 / Accepted: 9 February 2021 / Published online: 3 March 2021  
© The Author(s), under exclusive licence to Springer-Verlag London Ltd. part of Springer Nature 2021

## Abstract

Sustainable use of vegetable oil as a base fluid in minimum quantity lubrication (MQL) strategy for machining advanced materials is promising but limited due to their low thermal conductivity and viscosity. This paper presents the results of experimental investigation for enhancing viscosity and thermal conductivity of high oleic soybean vegetable oil (HOSO) using  $\text{Al}_2\text{O}_3$ ,  $\text{MoS}_2$ , and  $\text{TiO}_2$  nanoparticles (30 nm particle size and 0.5–4.0% wt. concentration) inclusion to form nanofluids at temperature ranging from 25 to 70 °C for use in vegetable oil-based nanofluids-MQL machining of difficult-to-cut metals. The result shows that viscosity and thermal conductivity of HOSO increase with increase in nanoparticle weight concentration, but there is a decrease in suspension stability of the nanofluid. Also, viscosity of HOSO nanofluids decreases with increase in temperature, but thermal conductivity increases with increase in temperature, while for the base HOSO, it decreases with increase in temperature. This is a very significant positive observation especially for difficult-to-cut materials that generate high heat that need to be conducted away from the cutting zone. Thermal conductivity and viscosity were enhanced up to 55% (using  $\text{MoS}_2$  at 70 °C and 4% wt. concentration) and 11.5% (using  $\text{TiO}_2$  at 50 °C and 3.5% wt. concentration), respectively. The Brownian motion of the nanoparticles and liquid-solid interlayer interfaces are responsible for this behavior of the nanofluid thermal conductivity, while nanoparticle thickening and entangle mechanism were responsible for the behavior of the nanofluid viscosity. This implies that lower oil flow rate can be applied during machining of Inconel-718 due to increased viscosity and thermal conductivity to obtain optimal machining performance, lower power consumption, and reduce negative impact on the environment.

**Keywords** Thermal conductivity · Viscosity · Nanofluid · High oleic soybean oil · Nanoparticles · Suspension stability

## Highlights

- Nanoparticle wt.% conc. in nanofluids follows similar Newtonian trend as HOSO fluid.
- $\text{TiO}_2$  nanoparticle results in maximum viscosity enhancement of HOSO base fluid.
- $\text{MoS}_2$  nanoparticle results in maximum thermal conductivity improvement of HOSO.
- Viscosity of  $\text{TiO}_2$ -,  $\text{MoS}_2$ -, and  $\text{Al}_2\text{O}_3$ -nanofluids decrease with increase in temperature.
- Thermal conductivity of the nanofluids increase with temperature and wt. % conc.

✉ Anthony C. Okafor  
okafor@mst.edu

<sup>1</sup> Computer Numerical Control and Virtual Manufacturing Laboratory, Department of Mechanical and Aerospace Engineering, Missouri University of Science and Technology, 327 Toomey Hall, Rolla, MO 65409-0050, USA

## 1 Introduction

Materials researchers are always looking for means to provide tougher materials used in engineering applications. These advanced materials need to be machined to their desired shape for specific applications. Cutting tools used during machining experience increased heat due to high friction and cutting forces generated at the cutting zone causing thermal softening of the cutting tool material, rapid tool wear, and shorter tool life. These adverse effects on the cutting tools also lead to reduced performance of the machined part due to reduced surface integrity such as high residual stresses and poor surface finish. Cutting fluids are used to improve surface integrity. The cutting fluid acts as a lubricant to reduce friction and as a coolant to cool the temperature at the cutting zone. Environmentally unfriendly conventional emulsion coolant (CEC) is the most effective cutting fluid for machining advanced materials like Inconel-718, titanium alloy, and

compacted iron graphite used in aerospace, nuclear, and automotive industries. Viscosity and thermal conductivity of fluids used in these applications are of utmost importance to researchers and manufacturers and determine the suitability of the cutting fluid. Theoretical models have been proposed for determining these intrinsic properties, but these properties are best obtained by experimental investigation [1–3] due to the limitation of available models.

*Nanofluids* have been proposed to be effective medium for transferring heat in applications such as heat exchangers, solar energy, and geothermal energy. Nanofluid is the suspension of nanoparticles in a base fluid to improve thermal conductivity of the base fluid. The base fluid predominantly reported in the literature is water, but vegetable oil is attracting a lot of interest due to its advantages over water. The nanoparticles could be metallic or non-metallic, and the nanofluid so formed could be conventional nanofluid (single type of nanoparticle of the same average size) or hybrid nanofluid (multi-type of nanoparticles of same or different average sizes). Pryazhnikov et al. [4] studied thermal conductivity of nanofluids using different volumes up to 8% concentrations of  $\text{SiO}_2$ ,  $\text{Al}_2\text{O}_3$ ,  $\text{TiO}_2$ ,  $\text{ZrO}_2$ , and  $\text{CuO}$  and diamond nanoparticle of varying sizes up to 150 nm at room temperature and using water, ethylene glycol, and engine oil as base fluids. After comparing their results with existing models, they concluded that thermal conductivity coefficient at room temperature is dependent on nanoparticle volume percentage, size, and property of the base-fluid. Asadi et al. [5] studied the effect of adding hybrid nanoparticles ( $\text{MgO}$ -MWCNT) to engine oil to form nanofluid. They showed that by increasing hybrid nanoparticle mass concentration to 2% and increasing temperature to 50 °C, thermal conductivity can be enhanced by 65%. Omrani et al. [6] studied thermal conductivity and viscosity of multi-walled carbon nanotubes with different length and outer diameter sizes using a volume fraction of 0.05% and deionized water as base fluid. The result showed an enhancement of 36% and 5.5% in the thermal conductivity and viscosity, respectively. Chandrasekar et al. [7] investigated thermal conductivity and viscosity of aluminum oxide/water nanofluid using 43 nm nanoparticle size at room temperature experimentally and theoretically. Nanofluid at different volume percentages was prepared using a microwave-assisted chemical precipitation method and dispersion using a sonicator. It was observed that thermal conductivity and viscosity increased with volume concentration. Turgut et al. [8] investigated the effect of  $\text{TiO}_2$  nanoparticles with deionized water as base fluid on thermal conductivity and viscosity measurement of the formed nanofluid. The result showed an increase in thermal conductivity of 7.4% at a volume concentration of 3% at a temperature of 13 °C. They also observed that the increase in viscosity was higher than that predicted using Einstein model. Vajjha and Das [9] experimentally investigated thermal conductivity of aluminum oxide, copper oxide, and zinc oxide nanofluids

using ethylene glycol and water mixture ratio 60:40 as base fluid. They also compared their results with those obtained using various existing models and observed that the results do not exhibit good agreement. Corcione [10] showed that effective thermal conductivity and dynamic viscosity of nanofluids are dependent on the size of the nanoparticle, base fluid, volume fraction of nanoparticle, and application temperature. These factors make it very difficult to use existing viscosity and thermal conductivity models to theoretically determine the effective thermal conductivity and viscosity of different nanofluids.

*Emulsion coolants* are formed by mixing soluble mineral-based oil with water and applied using pressure pumps to supply a large volume of the emulsion coolant at a rate usually from 300 to 3000 l/h to the cutting zone, which provides the necessary lubrication and transfer of heat away from the cutting zone when machining, especially difficult-to-cut materials [11]. The frequent use of emulsion coolant has an adverse effect on the environment, machine operators, and the economy. Mineral resources are non-renewable, proper disposal of used emulsion coolant is difficult and very expensive, and machining operators with respiratory and skin diseases have been known to be associated with constant exposure to mineral oil-based emulsion cutting fluids. The application of nanofluid in machining using emulsion coolant as base fluid is not feasible due to the large amount of fluid that is needed, the filtration system used during emulsion coolant application, and supplying the nanoparticle to the cutting zone will not be sustainable. Chetan et al. [12] investigated the application of alumina powder, colloidal solution of silver, and sunflower oil in water for use as nanofluid in turning process. They observed that nanoparticle affects the contact angle, surface tension, droplet size, and spreadability of the fluid which also reduce tool wear and cutting forces. The present need for sustainable, renewable, biodegradable, and environmentally friendly cutting fluids has been at the forefront of research in machining for decades. The use of vegetable oil has found its niche in machining materials such as mild steel and aluminum alloys in the form of minimum quantity lubrication (MQL).

*MQL* is the application of a small amount of oil supplied to the cutting zone with the aid of pressurized air to form atomized molecules of oil in the air. In MQL machining, the air pressure breaks a precise amount of oil into droplets. The aerosol applied to the cutting zone via a nozzle forms a lubricating film, inhibits friction and heat growth, and flushes the chips away from the cutting zone. These methods have been very effective in machining soft materials like mild steel and aluminum alloys. In cutting difficult-to-cut metals, problems are still experienced due to large amount of heat generated when machining materials like Inconel-718, compacted graphite iron, and titanium alloy. Recent studies have tried to solve such problems using cryogenic MQL [13–15], the application of cryogenic fluid in combination with MQL, or replacing pressurized shop air with

chilled air. These procedures are associated with hardening of the materials and further increase cutting forces and tool breakage due to sudden cooling.

Sidik et al. [16] conducted a review of nanofluid application in MQL, and it was observed that most application has been on soft materials like steel, aluminum, and pure titanium; the base fluid has been deionized water, ethyl-glycol, and ester oil. Behera et al. [17] investigated the spreadability of metalworking fluid using aluminum oxide and different surfactants in deionized water during turning. The improvement in machinability was observed to be due to the spreadability of the nanofluid. Yuan et al. [18] investigated the influence of copper, silicon carbide, and diamond nanoparticles in different vegetable oil for use as nanofluid in end-milling of aluminum alloy using MQL application. It was observed that the nanofluid show an improvement compared to dry machining by lowering cutting force and surface roughness. Li et al. [19] investigated the influence of graphene oxide nanofluid (graphene oxide suspended in commercially available synthetic ROCOL oil) on cutting temperature in machining Ti6Al4V. The result showed that the addition of nanoparticles reduced the cutting temperature and friction force.

*Vegetable oils* comprise mainly fatty acids that are either saturated or unsaturated. Saturated fatty acids have higher melting temperatures and most times solid at room temperature, while unsaturated fatty acids have low melting temperatures and tend to be liquid at room temperature. The viscosity and thermal conductivity of fluids used as load carrying fluid in moving parts and cooling medium in thermal applications are very important properties of the fluid. During machining of difficult-to-cut materials, the fluid in the cutting zone is subjected to shear stress and heat deformation due to shearing during chip formation. Viscosity and thermal conductivity of fluids are dependent on the shear rate and temperature. When machining difficult-to-cut metals such as Inconel-718, lower cutting speeds are used, and high cutting temperatures are generated compared to the not difficult-to-cut metals such as aluminum and steel. In MQL machining, the pressure and flow rate are very low compared to conventional emulsion flood cooling, therefore, the need to supply fluids with enhanced viscosity without inhibiting the fluidity of the fluid. A recent study shows that increasing oleic (unsaturated) fatty acids composition in soybean, vegetable oil can enhance the viscosity of soybean oil but not the thermal conductivity [20].

From the above literature reviewed, knowledge of the effect of nanoparticles on intrinsic properties of vegetable oil for use in machining difficult-to-cut metal is lacking and needs to be investigated. To enhance thermal conductivity of base vegetable oil for use in machining and understand its properties,  $\text{AlO}_3$ ,  $\text{TiO}_2$ , and  $\text{MoS}_2$  nanoparticles of 30 nm nanoparticle size were added and uniformly suspended in high oleic soybean oil (HOSO) to form  $\text{AlO}_3/\text{HOSO}$ -,  $\text{TiO}_2/\text{HOSO}$ -, and  $\text{MoS}_2/\text{HOSO}$  nanofluids to investigate the effect of type of

nanoparticle of the same nanoparticle size, weight concentration, temperature on shear stability, suspension stability, viscosity, and thermal conductivity before their application in MQL machining of difficult-to-cut metals. Nanofluid-MQL or minimum quantity nano-lubrication is the application of MQL with nanoparticles in the base fluid.

*High oleic soybean oil* has been shown to have the potential to replace mineral oil-based conventional emulsion flood coolant as a cutting fluid in the form of MQL application [21]. Modifying the fatty acid content of soybean oil is one method of increasing the viscosity of soybean oil. The method involves reducing the saturated fatty acid and polyunsaturated fatty acid contents which are solid at room temperature and have high oxidation rate, respectively. The method increases viscosity, oxidation stability, and shear stability without inhibiting the fluidity of the fluid. The influence of nanoparticles on rheological properties of nanofluid (viscosity and thermal conductivity) using high oleic soybean oil (HOSO) as base fluid has never been investigated, and most nanofluid study reported in the literature used water, engine oil, or ethyl-glycol as base fluids in other applications such as heat transfer fluids, most of which are limited to room temperature.

This study investigated the influence of three types of nanoparticles (titanium oxide ( $\text{TiO}_2$ ), M molybdenum disulfide ( $\text{MoS}_2$ ), and aluminum oxide ( $\text{Al}_2\text{O}_3$ )), varying nanoparticle weight concentration from 0.5 to 4% wt., and temperature range (25 to 70 °C) on shear stress, viscosity, thermal conductivity, and suspension stability of HOSO using the same 30 nm nanoparticle size in high oleic soybean vegetable oil as base fluid for potential use in nanofluids minimum quantity lubrication (nMQL) machining of difficult-to-cut materials.

## 2 Materials and method

### 2.1 Preparation of nanofluids

High oleic soybean vegetable oil (HOSO) was selected as a base fluid for comparative evaluation of three nanofluids based on our recent comparative study of high oleic soybean oil (HOSO), low oleic soybean oil (LOSO), Acculube 2000, and conventional emulsion flood coolant (CEFC) that showed the outstanding performance and potential of HOSO as cutting fluid for machining Inconel-718 using minimum quantity lubrication. Titanium oxide ( $\text{TiO}_2$ ), molybdenum disulfide ( $\text{MoS}_2$ ), and aluminum oxide ( $\text{Al}_2\text{O}_3$ ) nanoparticles were selected based on extensive literature review due to their compatibility with difficult-to-cut metals like Inconel-718 and their insolubility in the base vegetable oil. Uniform average nanoparticle size of 30 nm was selected based on the reported data in the literature on the effect of nanoparticle size that shows improvement in rheological properties of nanofluids with decrease in particle size, and 30 nm is the lowest

nanoparticle size that can be obtained across all nanoparticles investigated from nanoparticle manufacturers. The nanoparticle size of 30 nm was kept constant for all three nanoparticles to eliminate the influence of nanoparticle size on the result of the experiments. High oleic soybean oil was supplied by Archer Daniels Midland, USA. The nanoparticles used in the study were purchased from NANOSHEL, in the UK.

The varying weight percentage of nanoparticles from 0.5, 1, 1.5, 2.0, 2.5, 3.0, 3.5, and 4.0% and high oleic soybean oil were weighed using Torbal analytical balance with 0.0001 g accuracy. Each high oleic soybean oil with a measured weight percentage of nanoparticle was mixed mechanically and placed inside an ultrasonic bath for 2 h to disrupt the attraction between similar matter (liquid and solid) and further enhance solid-liquid mixture. After sonication, the mixture is mechanically mixed once again before each test is carried out.

## 2.2 Shear stress-shear rate and viscosity test

DHR II Rheometer from TA instrument was used to conduct the viscosity and shear stress-shear rate experiments on the HOSO base fluid and on the nanofluids as shown in Fig. 1. The DHR II was calibrated before each experiment using XHATCH – 40 mm parallel plate and Peltier plate. The experiments were conducted only after the calibration inertia, geometry inertia, friction, and gap temperature were within manufacturers' recommendation using a 700  $\mu\text{m}$  gap and 35  $\mu\text{m}$  trim gap offset (5% of the gap) to ensure proper loading and correct filling of the sample. The shear rate range was

selected based on a preliminary test with HOSO base fluid using 0 to 100 1/s shear rate range. The temperature of the HOSO base fluid and nanofluid for each test was set using the environment control temperature for DHR II from 25 to 70 °C. For each shear rate, the corresponding shear stress is obtained. The shear stress versus shear rate data were plotted, and the plots were then used to obtain the viscosity for the nanofluids and base fluid for a Newtonian fluid [20].

## 2.3 Thermal conductivity test

Thermal conductivity tests of the HOSO base fluid and nanofluids were conducted using a Thermtest TLS-100 portable thermal conductivity meter with ASTM and IEEE standards [20]. The transient line source meter uses a 100-mm needle sensor consisting of a thin heating wire and temperature sensor. The sensor was completely inserted into the sample tube placed in a water bath for varying temperature range from 25 to 70 °C; water bath heater was set to measurement temperature and allowed to stabilize; aluminum foils were used to control evaporation and cooling of the samples during thermal conductivity measurement, and experiments were conducted only when TLS-100 temperature sensor stabilizes. A constant current source was used to deliver heat to the sample, and the temperature rise is recorded over a period. Each measurement was repeated twice, and the average reading was used for results analysis.

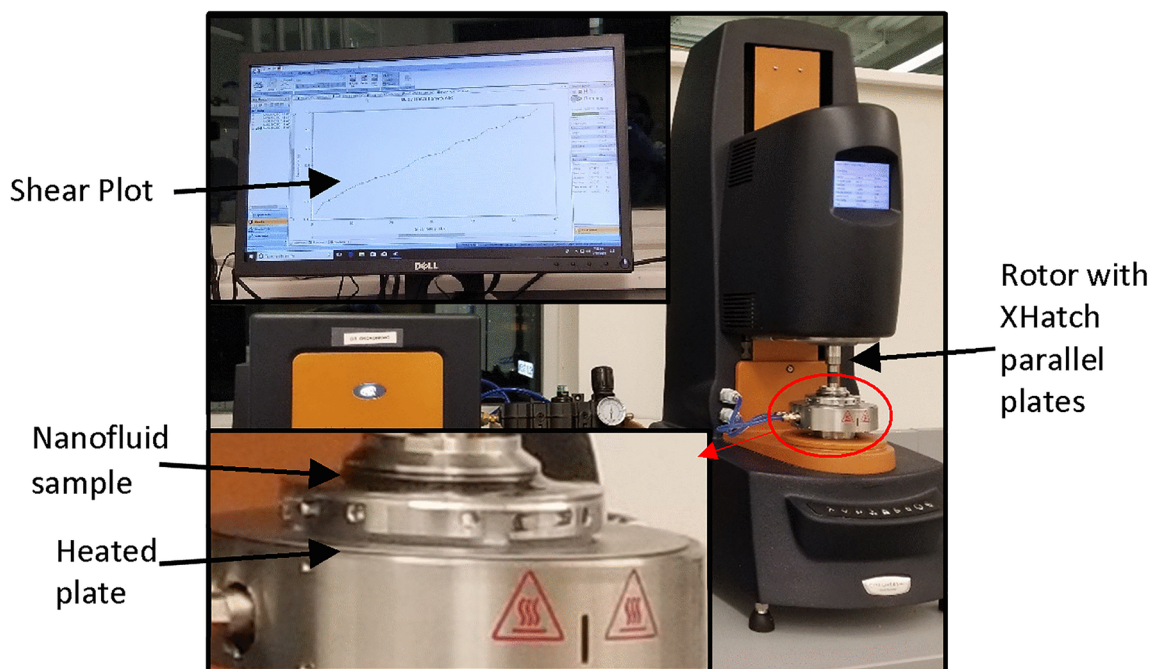


Fig. 1 Photograph of the experimental setup for rheology study using DHR-II

## 2.4 Suspension stability test

The suspension stability test of the nanofluids was done by physically monitoring the settling of the nanoparticles in the nanofluid over time. A camera was used to capture a picture of the physical state of the nanofluid, which was used for the analysis of the nanofluid suspension stability.

## 3 Results and discussion

### 3.1 Shear stress vs shear rate

A sample of the shear stress vs shear rate plots for HOSO base fluid,  $\text{Al}_2\text{O}_3/\text{HOSO}$ -,  $\text{TiO}_2/\text{HOSO}$ -, and  $\text{MoS}_2/\text{HOSO}$  nanofluids for 0.5 wt.% and 4.0 wt.% concentrations are shown in Figs. 2 and 3, respectively. The shear stresses were measured for shear rates ranging from 0 to 100 1/s. The shear stress vs shear rate plot of HOSO base fluid and all three investigated HOSO nanofluids ( $\text{Al}_2\text{O}_3/\text{HOSO}$ -,  $\text{TiO}_2/\text{HOSO}$ -, and  $\text{MoS}_2/\text{HOSO}$  nanofluids) for all nanoparticles, weight concentrations, and temperature showed similar linear trend typical for Newtonian fluid. As shown in Fig. 2 for 0.5 wt.%, shear stress increases linearly with increase in shear rate and decreases with increase in temperature for all three nanofluids. It is also observed that the shear stress of the nanofluids is more affected by temperature than by the type of nanoparticle. At shear rate of 100 1/s, nanofluids with 0.5 wt. % nanoparticle concentration generated shear stresses of 5.76, 5.62, and 5.70 Pa for  $\text{TiO}_2/\text{HOSO}$ ,  $\text{Al}_2\text{O}_3/\text{HOSO}$ , and  $\text{MoS}_2/\text{HOSO}$  nanofluids, respectively, at room temperature and 1.49, 1.44, and 1.47 Pa at 70 °C. All nanofluids showed similar shear stress, and the percentage increases were

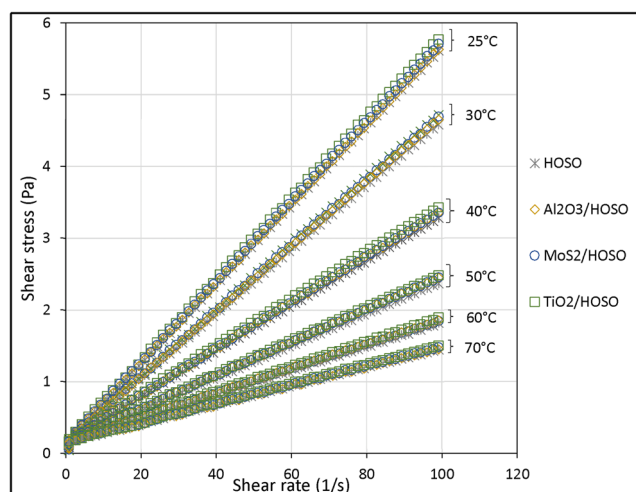


**Fig. 2** Shear stress vs shear rate of HOSO and  $\text{Al}_2\text{O}_3/\text{HOSO}$ ,  $\text{TiO}_2/\text{HOSO}$ , and  $\text{MoS}_2/\text{HOSO}$  nanofluids at 0.5 wt.% conc. and temperature from 25 to 70 °C

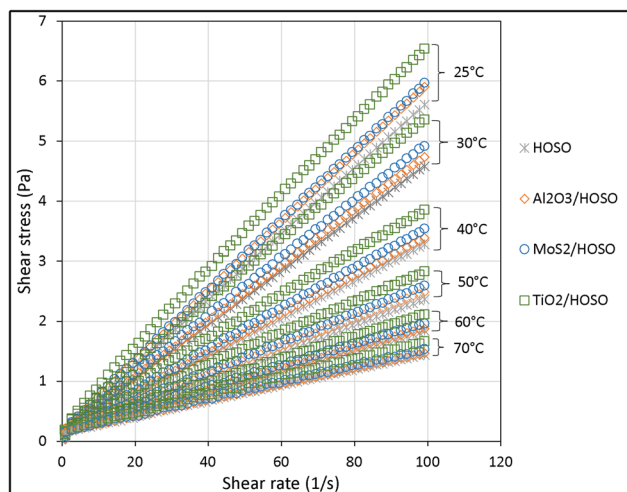


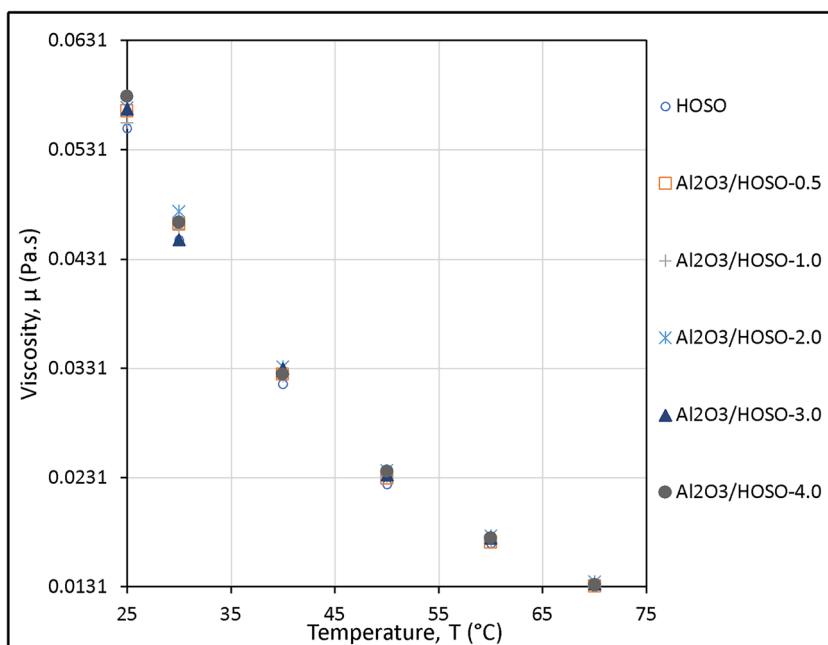
**Fig. 3** Shear stress vs shear rate of HOSO base fluid and  $\text{Al}_2\text{O}_3/\text{HOSO}$ ,  $\text{TiO}_2/\text{HOSO}$ , and  $\text{MoS}_2/\text{HOSO}$  nanofluids at 4.0 wt. % conc. and temperature from 25 to 70 °C

approximately equal compared to the base fluid, while the change in shear stress was observed to drop significantly due increase in temperature. At higher wt. % concentration as shown in Fig. 3, the proportionality of shear stress and shear rate is affected by type of nanoparticle and test temperature. It is observed that HOSO-based nanofluid using  $\text{TiO}_2$  nanoparticles has the highest shear stress and percentage increase from that of the base fluid. At 100 1/s shear rate, shear stresses of 6.53, 5.9, and 5.96 Pa were obtained for  $\text{TiO}_2/\text{HOSO}$ ,  $\text{Al}_2\text{O}_3/\text{HOSO}$ , and  $\text{MoS}_2/\text{HOSO}$  nanofluids, respectively, at room temperature and 1.66, 1.47, and 1.53 Pa at 70 °C. This is likely due to the mechanism behind functionality (association and entanglement and thickening mechanism) [22] on the type of nanoparticle and temperature as the wt. % concentration increases. Shear stress of HOSO nanofluids using  $\text{TiO}_2$ ,  $\text{MoS}_2$ , and  $\text{Al}_2\text{O}_3$  nanoparticles as additives increases comparatively to HOSO base fluid as nanoparticle wt. % concentration increases for a given shear rate and temperature. It can also be seen that  $\text{TiO}_2/\text{HOSO}$  nanofluid gave the highest shear stress followed closely by both  $\text{MoS}_2/\text{HOSO}$  and  $\text{Al}_2\text{O}_3/\text{HOSO}$  nanofluids. The shear stability of HOSO is not affected by the addition of nanoparticles for the range of wt. % concentrations and temperatures studied. The R square values were all above 0.99, showing a strong linear relationship between the shear stress and shear rate.

### 3.2 Viscosity and viscosity enhancement of base fluid

The plots of viscosity versus temperature of HOSO base fluid and HOSO nanofluids are shown in Figs. 4, 5, and 6 for  $\text{Al}_2\text{O}_3/\text{HOSO}$ ,  $\text{TiO}_2/\text{HOSO}$ , and  $\text{MoS}_2/\text{HOSO}$  nanofluids, respectively. The shear stress vs shear rate plots show a pattern like that of Newtonian fluids; therefore, viscosities were determined from the plots. Viscosities of HOSO base fluid and

**Fig. 4** Viscosity vs temperature for HOSO and Al<sub>2</sub>O<sub>3</sub>/HOSO nanofluid from 0.5 to 4.0 wt.% conc.



HOSO nanofluids were calculated using Eq. (1) for all shear stress vs shear rate line plots, for all three nanofluids at all nanoparticle wt. % concentration and temperature. The figures show that viscosity for HOSO base fluid and all three nanofluids decreases exponentially with the increase in temperature. Nanofluids with higher nanoparticle concentration show significant increase in viscosity compared to those with lower nanoparticle concentration and HOSO base fluid. The viscosity of Al<sub>2</sub>O<sub>3</sub>/HOSO, TiO<sub>2</sub>/HOSO, and MoS<sub>2</sub>/HOSO nanofluids and HOSO base fluid at room temperature shows

significant difference compared to those at 70 °C. This is likely due to the weakening of the solid-liquid interaction and reduction of the liquid shear stress leading to lower thickening and entanglement mechanism. Also, a significant difference is observed in the plots due to wt. % concentration increase at room temperature, and the differences decrease as temperature rises to 70 °C for TiO<sub>2</sub>/HOSO, compared to Al<sub>2</sub>O<sub>3</sub>/HOSO and MoS<sub>2</sub>/HOSO.

*Viscosity enhancement* of HOSO base fluid using TiO<sub>2</sub>, MoS<sub>2</sub>, and Al<sub>2</sub>O<sub>3</sub> nanoparticles as additives to the base fluid

**Fig. 5** Viscosity vs temperature for HOSO and TiO<sub>2</sub>/HOSO nanofluid from 0.5 to 4.0 wt.% conc.

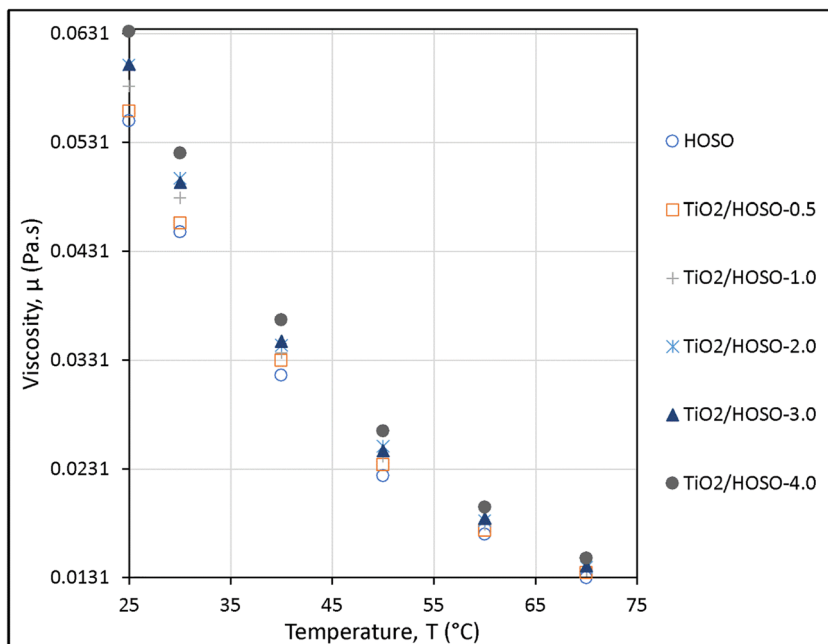
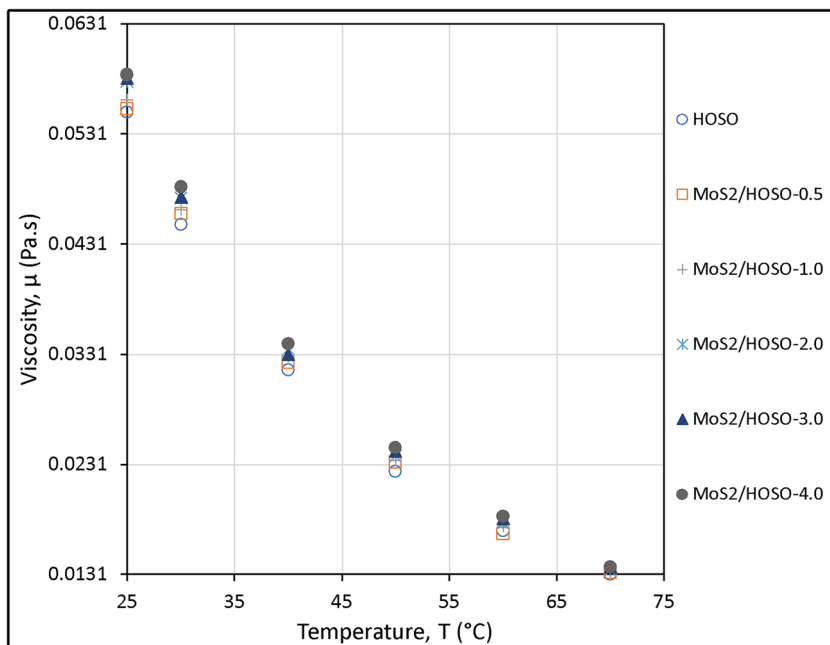


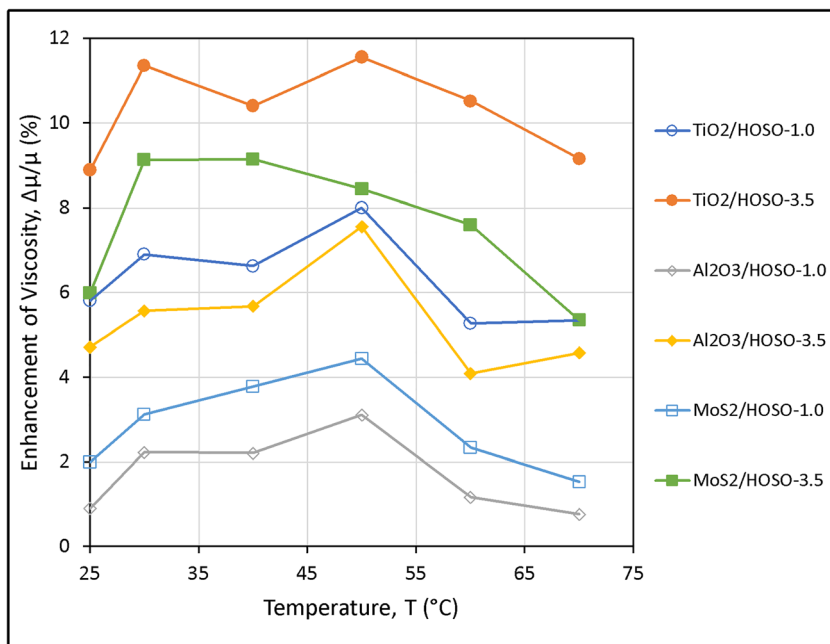
**Fig. 6** Viscosity vs temperature for HOSO and MoS<sub>2</sub>/HOSO nanofluid from 0.5 to 4.0 wt.% conc.



to form nanofluids is shown in Fig. 7 for 1.0 and 3.5 wt. % in nanoparticle concentrations. The viscosity enhancement of HOSO base fluid was calculated using Eq. (2) for nanoparticles and wt. % concentration at temperature range from 25 to 70 °C. An increase in wt. % concentration of nanoparticles leads to an increase in viscosity enhancement. Maximum viscosity enhancement of HOSO base fluid was obtained by using TiO<sub>2</sub> nanoparticles as additives which gave 11.5% and 8% enhancement at 3.5 and 1.0 wt. % concentration, respectively, at 50 °C, followed by using MoS<sub>2</sub> which gave 9.14% and 4.44% enhancement at 3.5 and 1.0 wt. % concentration, respectively, at 40 °C and 50 °C, and least enhancement occurred when Al<sub>2</sub>O<sub>3</sub> nanoparticle was used as additives in the base fluid which gave 7.5% and 3.1% at 3.5 and 1.0 wt. % concentration, respectively, at 50 °C. Figure 7 shows an increase in viscosity enhancement for a given wt. % concentration with an increase in temperature up to 50 °C and decreases with further increase in temperature. This can be

respective, at 50 °C, followed by using MoS<sub>2</sub> which gave 9.14% and 4.44% enhancement at 3.5 and 1.0 wt. % concentration, respectively, at 40 °C and 50 °C, and least enhancement occurred when Al<sub>2</sub>O<sub>3</sub> nanoparticle was used as additives in the base fluid which gave 7.5% and 3.1% at 3.5 and 1.0 wt. % concentration, respectively, at 50 °C. Figure 7 shows an increase in viscosity enhancement for a given wt. % concentration with an increase in temperature up to 50 °C and decreases with further increase in temperature. This can be

**Fig. 7** Viscosity enhancement vs temperature of HOSO base fluid using 1 and 3.5 wt. % nanoparticle concentration



explained by a combination of association and entanglement mechanism, thickening mechanism, solid-liquid interaction, and reduction of the liquid shear stress.

$$\sigma = \mu\gamma \quad (1)$$

$$\text{Enhancement}(\%) \Delta\mu / \mu = \frac{\mu_{\text{nanofluid}} - \mu_{\text{base fluid}}}{\mu_{\text{base fluid}}} \times 100 \quad (2)$$

( $\sigma$  is the shear stress (Pa),  $\gamma$  is the shear rate (1/s), and  $\mu$  is the dynamic viscosity (Pa. s).)

### 3.3 Thermal conductivity and thermal conductivity enhancement of base fluid

The plots of thermal conductivity vs temperature are shown in Figs. 8, 9, and 10 for Al<sub>2</sub>O<sub>3</sub>/HOSO-, TiO<sub>2</sub>/HOSO-, and MoS<sub>2</sub>/HOSO nanofluid, respectively. Equation (3) shows how thermal conductivity is obtained for both the based fluid and nanofluids. From the figures, thermal conductivity of HOSO base fluid decreases with a rise in temperature while that of nanofluids increases with a rise in temperature and an increase in nanoparticle weight concentration. The structure of fatty acid in HOSO and Brownian motion of free moving particles can be used to explain the above trend observed. HOSO acts as a heat sink, and temperature rise tends to break the fatty acid structure rather than moving the molecules, while in HOSO nanofluid, the movement and collision of free moving nanoparticles lead to energy transfer. Also, temperature rise decreases the viscosity of HOSO making it easier for nanoparticles to move within the

layers of HOSO in the nanofluid. The increase in the wt. % concentration increases clustering and bombardment of nanoparticles increasing heat transfer. It was observed that maximum thermal conductivity occurs at the maximum test temperature and nanoparticle wt. % concentration. Thermal conductivity was observed to be 0.275 w/mK for Al<sub>2</sub>O<sub>3</sub>/HOSO-, 0.271 w/mK for TiO<sub>2</sub>/HOSO-, and 0.276 w/mK for MoS<sub>2</sub>/HOSO nanofluids at 70 °C and 4.0 wt. % concentration. Thermal conductivity enhancement of HOSO nanofluid compared to the base fluid with an increase in temperature and nanoparticle wt.% concentration was obtained from Eq. (4) is shown in Fig. 11. The plot shows that increasing nanoparticle wt.% concentration increases the Brownian motion and collision of the particles and further enhances thermal conductivity of the nanofluids. Also, rise in temperature decreases viscosity of nanofluids and weakens the friction within the HOSO layers, thus causing an increase in the enhancement of nanofluid thermal conductivity. It was observed that thermal conductivity of HOSO can be enhanced to approximately 55% at temperature of 70 °C and by increasing the nanoparticle up to 4.0 wt. % concentration.

$$k = \frac{q}{4\pi a} \quad (3)$$

$$\text{Enhancement}(\%) \Delta k / k = \frac{k_{\text{nanofluid}} - k_{\text{base fluid}}}{k_{\text{base fluid}}} \times 100 \quad (4)$$

( $k$  is the thermal conductivity (w/mK),  $q$  is the quantity of heat supplied, and  $a$  is the slope of temperature rise over a logarithm time.)

**Fig. 8** Thermal conductivity vs temperature for HOSO and Al<sub>2</sub>O<sub>3</sub>/HOSO nanofluid from 0.5 to 4.0 wt.% conc.

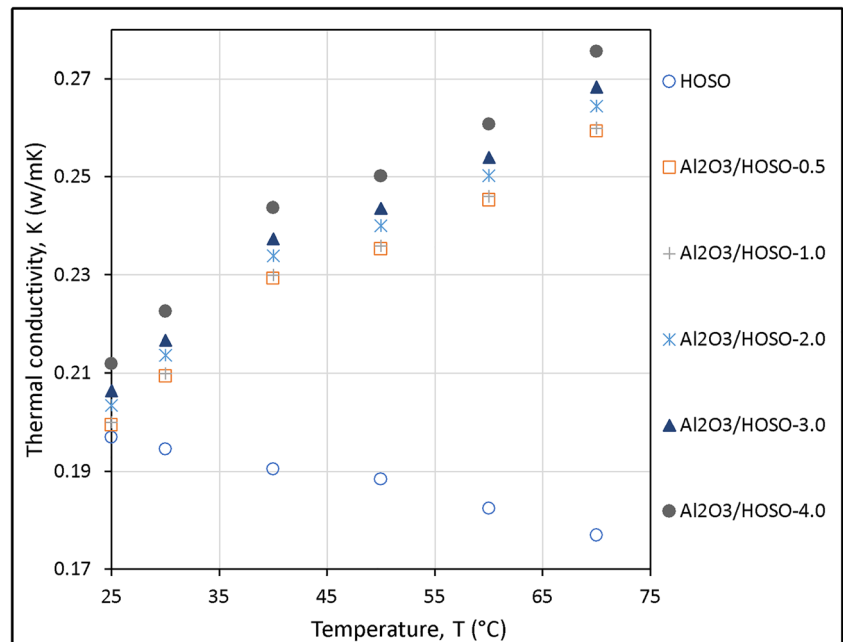
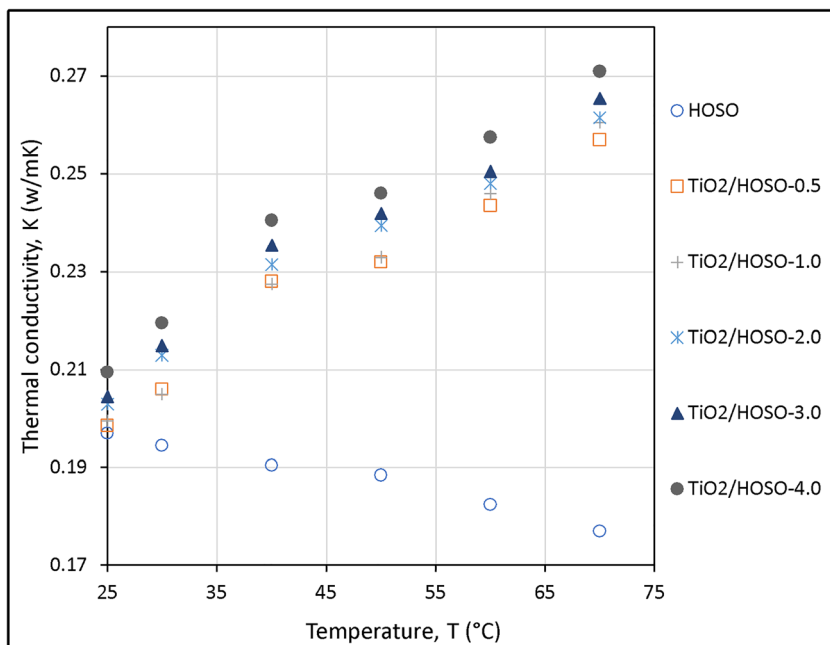




**Fig. 9** Thermal conductivity vs temperature for HOSO and TiO<sub>2</sub>/HOSO nanofluid from 0.5 to 4.0 wt.% conc.



### 3.4 Suspension stability

The nanoparticle suspension stability is shown in Fig. 12, for Al<sub>2</sub>O<sub>3</sub>/HOSO-, MoS<sub>2</sub>/HOSO-, and TiO<sub>2</sub>/HOSO nanofluid using 0.5, 2.0, and 4.0 wt.% concentration, respectively. The nanoparticles were observed to be stable for all weight concentrations up to 1 h except for TiO<sub>2</sub>-HOSO at 4.0 wt.% concentration. It was also observed that nanoparticle suspension stability decreases with an increase in wt.%

concentration. This trend can be possible due to the larger mass in the nanofluid, causing nanoparticles to push through the base fluid layers and agglomerate easily. Al<sub>2</sub>O<sub>3</sub>/HOSO nanofluid was stable for up to 3 days and started agglomeration for larger weight concentration. MoS<sub>2</sub>/HOSO nanofluid maintained its stability and started agglomerating after 1 week and completely settled at 2 weeks. MoS<sub>2</sub> showed longer stability in HOSO compared to Al<sub>2</sub>O<sub>3</sub>, and TiO<sub>2</sub> showed the lowest stability in HOSO.

**Fig. 10** Thermal conductivity vs temperature for HOSO and MoS<sub>2</sub>/HOSO nanofluid from 0.5 to 4.0 wt.% conc.

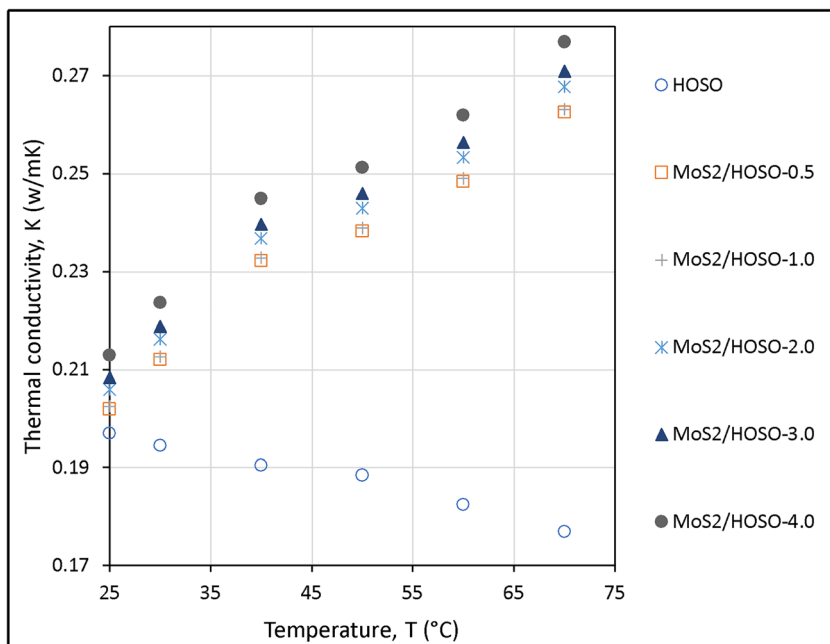
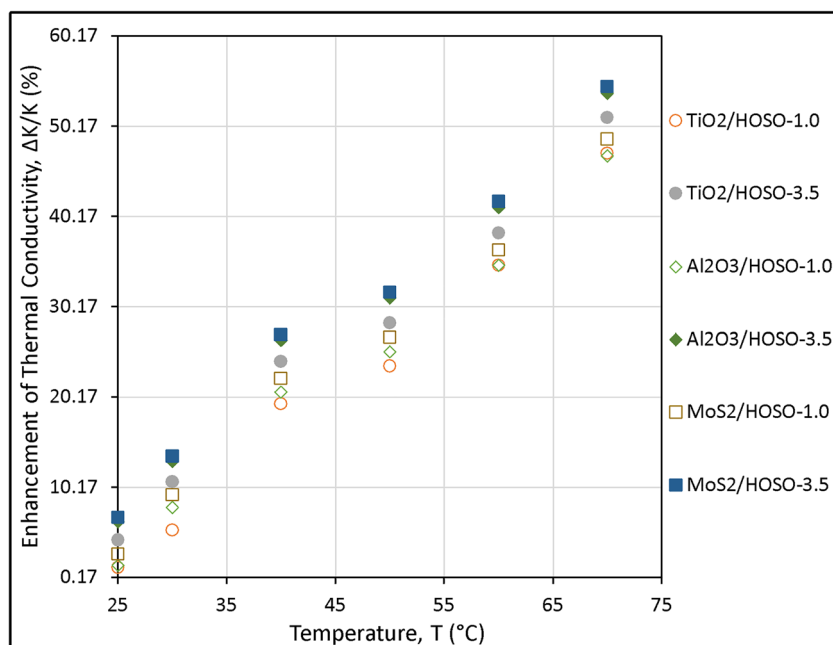


**Fig. 11** Enhancement of thermal conductivity vs temperature of  $\text{Al}_2\text{O}_3/\text{HOSO}$ ,  $\text{TiO}_2/\text{HOSO}$ , and  $\text{MoS}_2/\text{HOSO}$  nanofluid for 1.0 to 3.5 wt.% conc.

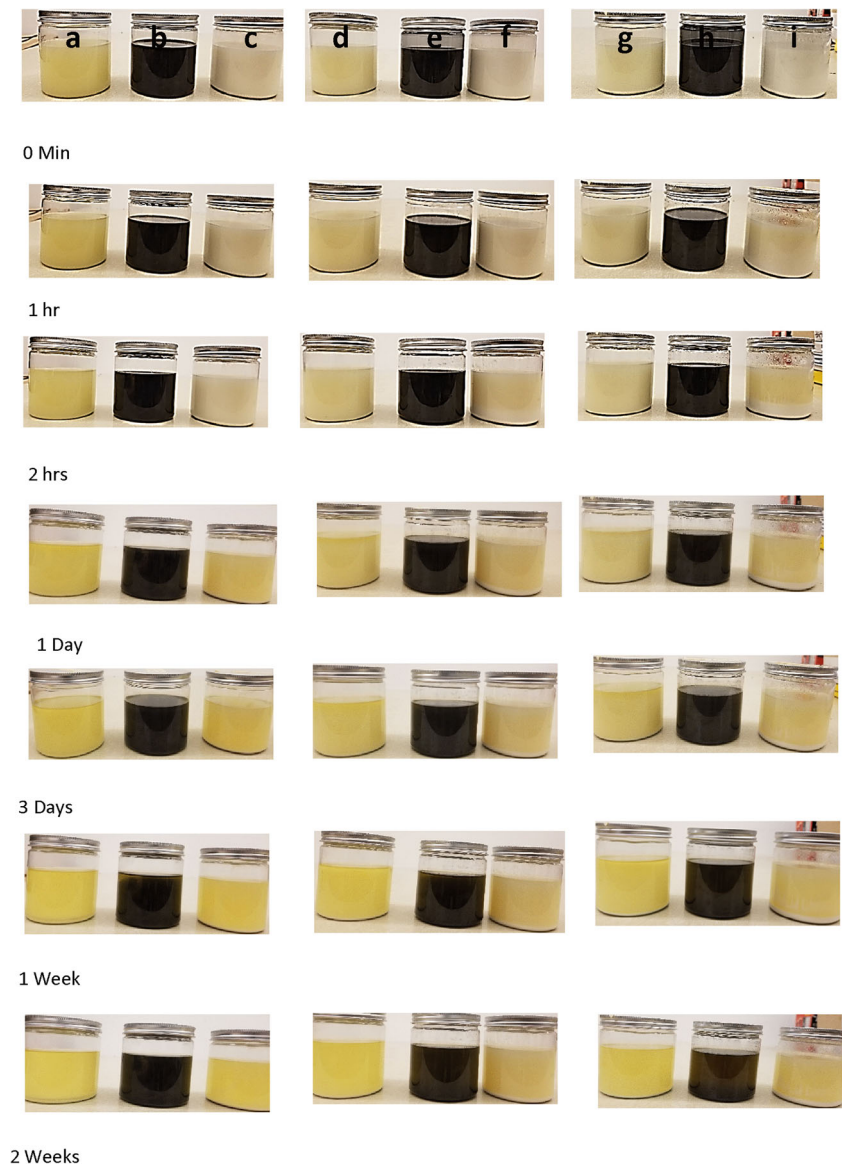


## 4 Conclusions

This study investigated shear stress vs shear rate, viscosity, thermal conductivity, and suspension stability of three vegetable oil-based nanofluids using high oleic soybean oil (HOSO) as the base fluid and  $\text{Al}_2\text{O}_3$ ,  $\text{MoS}_2$ , and  $\text{TiO}_2$  nanoparticles of same 30 nm average nanoparticle size at varying weight concentration (0.5–4% wt.) and temperature range from 25 to 70 °C, for use as cutting fluids in nanofluid minimum quantity lubrication (nMQL) machining of difficult-to-cut metals. The resulting nanofluids are designated as  $\text{TiO}_2/\text{HOSO}$ ,  $\text{MoS}_2/\text{HOSO}$ , and  $\text{Al}_2\text{O}_3/\text{HOSO}$  nanofluids. From the results, the following conclusions are made.

1. Shear stress vs shear rate plots of  $\text{TiO}_2/\text{HOSO}$ ,  $\text{MoS}_2/\text{HOSO}$ , and  $\text{Al}_2\text{O}_3/\text{HOSO}$  nanofluids show increasing linear trend typical of Newtonian fluids for all temperature range and percentage weight concentration investigated.
2. Shear stress of  $\text{TiO}_2/\text{HOSO}$ ,  $\text{MoS}_2/\text{HOSO}$ , and  $\text{Al}_2\text{O}_3/\text{HOSO}$  nanofluids decreases exponentially with increase in temperature.
3.  $\text{TiO}_2/\text{HOSO}$  nanofluid generates the highest shear stress followed by  $\text{MoS}_2/\text{HOSO}$ ,  $\text{Al}_2\text{O}_3/\text{HOSO}$ , and HOSO base fluid in that order for all temperature and nanoparticle wt.% concentration; and shear stress increases with increase in nanoparticle wt. concentration, the highest increase occurring at room temperature (25 °C).
4. Viscosity of  $\text{TiO}_2/\text{HOSO}$ ,  $\text{MoS}_2/\text{HOSO}$ , and  $\text{Al}_2\text{O}_3/\text{HOSO}$  nanofluids and HOSO base fluid decreases exponentially with increase in temperature, and they increase with increase in nanoparticle % wt. concentration from 0 to 4% wt.
5. Viscosity of HOSO base fluid can be enhanced using  $\text{TiO}_2$ ,  $\text{MoS}_2$ , and  $\text{Al}_2\text{O}_3$  nanoparticles as additives to form nanofluids.
6. Maximum viscosity enhancement of HOSO base fluid is obtained by using  $\text{TiO}_2$  nanoparticles as additive to provide up to 11.5% and 8% enhancement at 3.5% wt. and 1% wt. concentration, respectively, at 50 °C;  $\text{MoS}_2$  nanoparticles can provide up to 9.14% and 4.44% enhancement at 3.5% wt. and 1% weight concentration at 50 °C, respectively, while  $\text{Al}_2\text{O}_3$  nanoparticles provide the least enhancement of 7.5% and 3.1% at 3.5% wt. and 1% wt. concentration, respectively, at 50 °C.
7. Thermal conductivity of  $\text{TiO}_2/\text{HOSO}$ -,  $\text{MoS}_2/\text{HOSO}$ -, and  $\text{Al}_2\text{O}_3/\text{HOSO}$  nanofluids increases with increase in temperature and nanoparticle wt. concentration, while thermal conductivity of HOSO base fluid decreases with increase in temperature. This is very significant positive observation especially for machining difficult-to-cut metals that generate high heat that need to be conducted away from the cutting zone.
8. Maximum thermal conductivity occurs at 70 °C and 4% wt. concentration for all three nanofluids investigated.
9. Maximum thermal conductivity enhancement of HOSO base fluid is obtained by using  $\text{MoS}_2$  nanoparticles as

**Fig. 12** Suspension stability of nanoparticles in nanofluid at 0.5, 2.0, and 4.0 wt.% conc. (a  $\text{Al}_2\text{O}_3/\text{HOSO}$ -0.5%, b  $\text{MoS}_2/\text{HOSO}$ -0.5%, c  $\text{TiO}_2/\text{HOSO}$ -0.5%, d  $\text{Al}_2\text{O}_3/\text{HOSO}$ -2.0%, e  $\text{MoS}_2/\text{HOSO}$ -2.0%, f  $\text{TiO}_2/\text{HOSO}$ -2.0%, g  $\text{Al}_2\text{O}_3/\text{HOSO}$ -4.0%, h  $\text{MoS}_2/\text{HOSO}$ -4.0%, i  $\text{TiO}_2/\text{HOSO}$ -4.0%)



additive which provides up to 55% enhancement at 70 °C and 4% wt., followed by  $\text{Al}_2\text{O}_3/\text{HOSO}$  and then  $\text{TiO}_2/\text{HOSO}$  nanofluids.

10. Maximum thermal conductivities obtained were 0.276, 0.275, and 0.271 for  $\text{MoS}_2/\text{HOSO}$ -,  $\text{Al}_2\text{O}_3/\text{HOSO}$ -, and  $\text{TiO}_2/\text{HOSO}$  nanofluids, respectively, at 70 °C and 4% wt. concentration.
11. Since of significant interest is enhancement of thermal conductivity of HOSO vegetable oil,  $\text{MoS}_2/\text{HOSO}$  nanofluid is recommended followed by  $\text{Al}_2\text{O}_3/\text{HOSO}$  nanofluid and then  $\text{TiO}_2/\text{HOSO}$  nanofluid.
12.  $\text{MoS}_2$  nanoparticle remains stable in high oleic soybean oil for about 2 weeks, and it is more stable compared to  $\text{Al}_2\text{O}_3$  nanoparticle and  $\text{TiO}_2$  nanoparticle which exhibit the lowest suspension stability in HOSO. The increase in

nanoparticle weight concentration leads to poor suspension stability of the nanofluid.

13. To further enhance viscosity and thermal conductivity of high oleic soybean oil, the authors propose to investigate  $\text{MoS}_2$ ,  $\text{Al}_2\text{O}_3$ ,  $\text{TiO}_2$ , and graphene nanofluids by extending nanoparticle weight concentration up to 8%.

**Acknowledgements** The authors appreciate the assistance of Dr. Monday Okoronkwo and Dr. Muthanna H. Al-Dahhan in the Department of Biomedical and Chemical Engineering at Missouri S & T for providing the rheology and thermal conductivity equipment respectively used for the experiments.

**Funding** This study received financial support from the Intelligent System Center (ISC) and the Advanced Manufacturing Signature Area (AMS) at Missouri University of Science and Technology and financial

assistance in the form of Graduate Teaching Assistantship by the Department of Mechanical and Aerospace Engineering at Missouri University of Science and Technology.

**Availability of data and material** Not applicable

**Code availability** Not applicable

## Declarations

**Competing interests** The authors declare no competing interests.

## References

- Ahmadi MH, Mirlohi A, Alhuyi Nazari M, Ghasempour R (2018) A review of thermal conductivity of various nanofluids. *J Mol Liq* 265:181–188
- Mishra PC, Mukherjee S, Nayak SK, Panda A (2014) A brief review on viscosity of nanofluids. *Int Nano Lett* 4:109–120. <https://doi.org/10.1007/s40089-014-0126-3>
- Bashirmezahd K, Bazri S, Safaei MR, Goodarzi M, Dahari M, Mahian O, Dalkılıça AS, Wongwises S (2016) Viscosity of nanofluids: a review of recent experimental studies. *Int Commun Heat Mass Transf* 73:114–123. <https://doi.org/10.1016/j.icheatmasstransfer.2016.02.005>
- Pryazhnikov MI, Minakov AV, Rudyak VY, Guzei DV (2017) Thermal conductivity measurements of nanofluids. *Int J Heat Mass Transf* 104:1275–1282. <https://doi.org/10.1016/j.jheatmasstransfer.2016.09.080>
- Asadi M, Asadi A, Aberoumand S (2018) An experimental and theoretical investigation on the effects of adding hybrid nanoparticles on heat transfer efficiency and pumping power of an oil-based nanofluid as a coolant fluid. *Int J Refrig* 89:83–92. <https://doi.org/10.1016/j.ijrefrig.2018.03.014>
- Omran AN, Esmailzadeh E, Jafari M, Behzadmehr A (2019) Effects of multi walled carbon nanotubes shape and size on thermal conductivity and viscosity of nanofluids. *Diam Relat Mater* 93:96–104. <https://doi.org/10.1016/j.diamond.2019.02.002>
- Chandrasekar M, Suresh S, Chandra Bose A (2010) Experimental investigations and theoretical determination of thermal conductivity and viscosity of Al<sub>2</sub>O<sub>3</sub>/water nanofluid. *Exp Thermal Fluid Sci* 34:210–216. <https://doi.org/10.1016/j.expthermflusci.2009.10.022>
- Turgut A, Tavman I, Chirtoc M, Schuchmann HP, Sauter C, Tavman S (2009) Thermal conductivity and viscosity measurements of water-based TiO<sub>2</sub> nanofluids. *Int J Thermophys* 30:1213–1226. <https://doi.org/10.1007/s10765-009-0594-2>
- Vajjha RS, Das DK (2009) Experimental determination of thermal conductivity of three nanofluids and development of new correlations. *Int J Heat Mass Transf* 52:4675–4682. <https://doi.org/10.1016/j.jheatmasstransfer.2009.06.027>
- Corcione M (2011) Empirical correlating equations for predicting the effective thermal conductivity and dynamic viscosity of nanofluids. *Energy Convers Manag* 52–1:789–793. <https://doi.org/10.1016/j.enconman.2010.06.072>
- Ezugwu EO, Bonney J (2004) Effect of high-pressure coolant supply when machining nickel-base, Inconel 718, alloy with coated carbide tools. *J Mater Process Technol* 153–154:1045–1050. <https://doi.org/10.1016/j.jmatprotec.2004.04.329>
- Chetan BBC, Ghosh S, Rao PV (2016) Application of nanofluids during minimum quantity lubrication: a case study in turning process. *Tribol Int* 101:234–246. <https://doi.org/10.1016/j.triboint.2016.04.019>
- Shokrani A, Dhokia V, Newman ST (2016) Investigation of the effects of cryogenic machining on surface integrity in CNC end milling of Ti-6Al-4V titanium alloy. *J Manuf Process* 21:172–179. <https://doi.org/10.1016/j.jmapro.2015.12.002>
- Park KH, Suhaimi MA, Yang GD, Lee DY, Lee SW, Kwon P (2017) Milling of titanium alloy with cryogenic cooling and minimum quantity lubrication (MQL). *Int J Precis Eng Manuf* 18:5–14. <https://doi.org/10.1007/s12541-017-0001-z>
- Okafor AC, Jasra PM (2019) Effects of milling methods and cooling strategies on tool wear, chip morphology and surface roughness in high speed end-milling of inconel-718. *Int J Mach Mach Mater* 21:3. <https://doi.org/10.1504/ijmmm.2019.098065>
- Sidik NAC, Samion S, Ghaderian J, Yazid MNAWM (2017) Recent progress on the application of nanofluids in minimum quantity lubrication machining: a review. *Int J Heat Mass Transf* 108:79–89
- Behera BC, Chetan, Setti D et al (2017) Spreadability studies of metal working fluids on tool surface and its impact on minimum amount cooling and lubrication turning. *J Mater Process Technol* 244:1–16. <https://doi.org/10.1016/j.jmatprotec.2017.01.016>
- Yuan S, Hou X, Wang L, Chen B (2018) Experimental investigation on the compatibility of nanoparticles with vegetable oils for nanofluid minimum quantity lubrication machining. *Tribol Lett* 66. <https://doi.org/10.1007/s11249-018-1059-1>
- Li G, Yi S, Li N, Pan W, Wen C, Ding S (2019) Quantitative analysis of cooling and lubricating effects of graphene oxide nanofluids in machining titanium alloy Ti6Al4V. *J Mater Process Technol* 271:584–598. <https://doi.org/10.1016/j.jmatprotec.2019.04.035>
- Okafor AC, Nwoguh TO (2020) A study of viscosity and thermal conductivity of vegetable oils as base cutting fluids for minimum quantity lubrication machining of difficult-to-cut metals. *Int J Adv Manuf Technol* 106:1121–1131. <https://doi.org/10.1007/s00170-019-04611-3>
- Okafor AC, Nwoguh TO (2020) Comparative evaluation of soybean oil-based MQL flow rates and emulsion flood cooling strategy in high-speed face milling of Inconel 718. *Int J Adv Manuf Technol* 107:3779–3793. <https://doi.org/10.1007/s00170-020-05248-3>
- Martini A, Ramasamy US, Len M (2018) Review of viscosity modifier lubricant additives. *Tribol Lett* 66:58, 1–14. <https://doi.org/10.1007/s11249-018-1007-0>

**Publisher's note** Springer Nature remains neutral with regard to jurisdictional claims in published maps and institutional affiliations.